International Journal of Integrated Engineering, Vol. 10 No. 4 (2018) p. 88-94

DOI: https://doi.org/10.30880/ijie.2018.10.04.014

Numerical Simulation of Concentration Over-voltage in a Polymer Electrolyte Fuel Cell under Low-Hydrogen Conditions

Takahisa Yamamoto[1,*], Kazuhiro Ishimaru[1], Kahar Osman[2], Mohamad Ikhwan Kori[2], Ahmad Zaharan Khudzari[2], Ishkrizat Taib[3], Tsuyoshi Yamamoto[4]

[1]Department of Mechanical Engineering, National Institute of Technology, Gifu College, Motosu 501-0495, JAPAN.
[2]IJN-UTM Cardiovascular Engineering Centre, Universiti Teknologi Malaysia, Skudai 81310, Malaysia.
[3]Department of Energy and Thermofluid Engineering, Universiti Tun Hussein Onn Malaysia, Johor 86400 Malaysia.
[4]Department of Chemical Engineering, Kyushu University, Fukuoka 819-0395, JAPAN.

Received 7 March 2018; accepted 30 May 2018, available online 6 August 2018

Abstract: This article elucidates the effect of low hydrogen concentration fuel gas on polymer electrolyte fuel cell (PEFC) performance, with particular emphasis on the transport of chemical species in the anode separator channel and the electrochemical reactions. A numerical simulation model for PEFCs was developed; the model combined a computational fluid dynamics model for mass transfer in the anode separator and the gas diffusion layer (GDL) as well as a PEFC electrochemical reaction model taking into account the activation, concentration, and resistance over-voltages. The emphasis in this study is placed on obtaining a basic understanding of how three-dimensional flow and low-hydrogen fuel transport phenomena in the anode separator channel impact the electrochemical processes occurring in PEFCs. Comparison of the numerical simulation results with experimental data indicates that the performance degradation in PEFCs is negligible for hydrogen concentrations over 30%, whereas it becomes significant for concentrations below 10%. Furthermore, the numerical simulation results show that controlling the fuel supply flow rate stimulates hydrogen transport in the GDL and the catalyst layer, which consequently enhances PEFC performance under low-hydrogen conditions.

Keywords: Polymer electrolyte fuel cell, concentration over-voltage, computer fluid dynamics, electrochemical reaction model, Low hydrogen fuel gas fuel

1. Introduction

Polymer electrolyte fuel cells (PEFCs), which are candidate next-generation energy conversion systems, have low operating temperatures and high power densities compared with other types of fuel cells. A conventional PEFC system uses fuel gas with a hydrogen concentration as high as 90 vol.% [1]. One hydrogen production method for PEFC fuel gas is biomass or fossil fuel gasification [2,3]. This production method produces not only hydrogen but also impurity gases such as carbon monoxide and carbon dioxide. Therefore, a purification process is required to separate hydrogen from the other impurity gases. Current purification processes employ a pressure swing adsorption method or a membrane isolation method. However, these purification processes consume a large amount of production energy, consequently yielding high production costs [4,5].

To improve PEFC power generation performance with low hydrogen concentration fuel gas, it is important to optimize PEFC operating conditions and design separator channels with a geometry that satisfies the following condition: the current density distribution and chemical species distributions are unified. There are a few reports on the optimization of PEFC operating conditions and the design of gas flow channels under low hydrogen concentration conditions [6]. As the flow and mass transfer phenomena between microscopic and macroscopic areas are complex, it is very difficult to visualize and measure PEFC performance experimentally. Some researchers have developed numerical analysis models to examine PEFC performance. Recently, PEFC analysis models employing a computational fluid dynamics (CFD) technique to calculate the transport phenomena of chemical species have been reported in detail [7-13]. Zhou and Hashemi developed a finite volume method for studying multicomponent transport in porous electrodes [14,15]. Kopanidis and Taymaz developed a three-dimensional model and analyzed large-scale PEFCs with actual serpentine flow field [16,17]. However, these studies did not focus on PEFC characteristics under conditions of low hydrogen concentration.

In the present work, a PEFC analysis model employing three-dimensional CFD was developed to analyze current density and hydrogen concentration distributions, and the effect of low hydrogen concentration on PEFC performance with a serpentine channel was

*Corresponding author: ytaka@gifu-nct.acjp

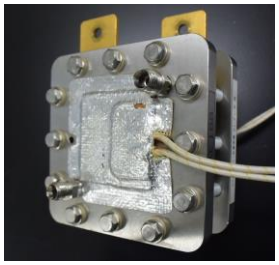

(a) PEFC cell

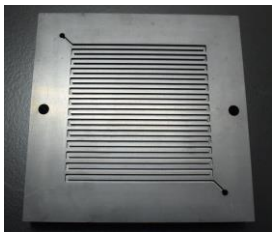

(b) Anode separator channel

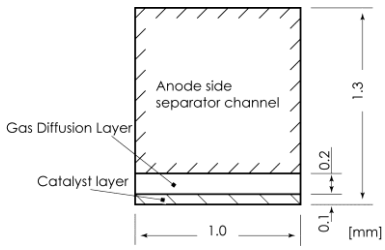

(c) cross section of anode separator channel

Figure 1: PEFC and separator channel

discussed. This study also analyzed U-type channel flow to confirm the accuracy of the fluid flow model, and PEFC performance tests were performed to validate the electrochemical reaction model.

2. PEFC and Anode Separator Channel

Schematics of a PEFC and the anode separator channel are shown in Figure 1. This study used a single standard cell developed by Japan Automobile Research Institute. The area of the cell membrane was 50 mm × 50 mm. The width and height of each channel were 1.0 mm and 1.3 mm, respectively. The channel comprises a gas diffusion layer (GDL) with a depth of 0.2 mm and a catalyst layer with a depth of 0.1 mm. NAFION-12, which based on platinum, was used as a catalyst in the catalyst layer, and its volume fraction was 0.1. The fuel gas, which comprises a mixture of hydrogen and nitrogen, flows from the channel inlet to the outlet. At the same time, hydrogen diffuses through the GDL and into the catalyst layer. Electrochemical reactions then occur on the surface of the catalyst, and hydrogen is consumed and converted into protons and electrons.

3 Numerical Model of PEFC

This study developed a PEFC analysis model comprising two parts: one is a three-dimensional CFD model for the anode separator channel, and the other is an electrochemical reaction model. In the CFD model, equations of continuity, momentum, and mass balance in both the anode separator channel and the GDL are calculated using a finite difference method. In the electrochemical reaction model, this present work extends a model developed by Inoue et al.[17,18] The present PEFC analysis model makes the following assumptions:

- The effective porosity and permeability are uniform in the GDL;
- The heat of reaction is discharged out of the PEFC, and the temperature of the PEFC is constant at 353 K;
- Water produced by electrochemical reactions and humidified water exist as vapor. Reaction area reduction caused by flooding and diffusion prevention caused by water condensation are also ignored;
- The partial pressures of water in the humidified gases are equal to the saturated vapor pressure;
- The electrolyte membrane is well humidified, and the ionic conductivity is constant and uniform;
- Gas crossover is disregarded;
- The cell voltage is uniform;
- The gas concentrations either side of the interface between the gas flow channel and the GDL are equal;

The fluids are incompressible Newtonian fluids and ideal gases. The flow conditions are laminar flow.

3.1 Governing Equations of CFD

The equation of continuity is written as

$$\frac{\partial \rho}{\partial t} + \nabla \cdot (\rho \bar{U}) = 0, \tag{1}$$

where ρ and $\bar{U}$ are the density and velocity vector of the fuel gas, respectively. The equation of motion in the GDL and the separator channel is

$$\frac{\partial \bar{U}}{\partial t} + \nabla \cdot (\rho \bar{U}\bar{U}) = -\nabla p + \nabla(\mu \nabla \bar{U}) + Su, \tag{2}$$

where p and μ are the gas pressure and viscosity, respectively. Su is a source term in the equation of motion that expresses pressure losses in the porous media, GDL, and catalyst layer and is given by

$$Su = -\frac{\mu}{K} f_a^2 \bar{U}, \tag{3}$$

where K and f_a are the permeability and porosity of the GDL, respectively. The transport equation of chemical species is written as

$$\frac{\partial Y_i}{\partial t} + \nabla \cdot (\bar{U} Y_i) = \nabla \cdot (D_i^{eff} Y_i) + S_{Y_i}, \tag{4}$$

where Y_i denotes the mass fraction of chemical species i and S_{Yi} expresses the consumption rate of chemical species i. D_i^{eff} is the effective diffusion coefficient of the fuel gas and can be calculated as

$$D_i^{eff} = D_i f_a^{\tau}, \tag{5}$$

where D_i is the diffusion coefficient of chemical species i, f_a is the effective porosity of the anode, and τ is the

Table 1. Fitting parameters

Effective porosity of anode, f_a	Effective porosity of cathode, f_c	Transfer coefficient of anode, α_a	Transfer coefficient of cathode, $\alpha_{1,c}$	Model constant in activation over-voltage, C_α
0.02	0.043	0.10	0.09	0.98

Table 2. Physical parameters of PEFC

Supplied pressure, P	101.3 kPa
Standard electromotive force, E_0	1.23 V
Operating voltage, E	0.5 V
Diffusion coefficient of H_2, D_{H2O}	1.03×10^{-4} m^2/s
Diffusion coefficient of O_2, D_{O2}	2.91×10^{-5} m^2/s
Number of electrons participating reaction, n	2
Ratio of platinum in catalyst, P_t	10%
Depth of membrane, t_m	30 µm
Depth of GDL, l	300 µm

tortuosity factor. The fuel gas is treated as an ideal gas that obeys

$$pv = nRT. \tag{6}$$

3.2 Electrochemical Reaction Model

In this study, the operation voltage (V) is calculated using the following equation:

$$V = E - \eta_{act,a} - \eta_{act,c} - \eta_{con,a} - \eta_{con,c} - \eta_{ohm,m}, \tag{7}$$

where E is the electromotive force, η_{act} is the activation over-voltage, η_{con} is the concentration over-voltage, η_{ohm} is the resistance over-voltage, and the subscripts a, c, and m represent the anode, the cathode, and the membrane, respectively. In this study, the following parameters affecting these over-voltages were used as fitting parameters so that the calculation results agreed with the experimental data under various conditions; f_a is the effective porosity of the anode side GDL, f_c is the effective porosity of the cathode side GDL, α_a is the transfer coefficient of the anode side concentration over-voltage, C_α is the coefficient to calculate the transfer coefficient of the activation over-voltage, C_σ and k_σ are the correction coefficients to calculate the membrane ionic conductivity, and k_{io} is the correction coefficients to calculate the exchange current density. Although some assumptions and aspects of the models are not strict theoretically, the following models were developed only to use these values as fitting parameters. The details of these over-voltages are given in the following sections.

3.2.1 Electromotive force

The electromotive force is calculated by means of the following Nernst equation:

$$E = E_0 + \frac{RT}{nF} \ln\left[\frac{P_{H_2,a} \cdot (P_{O_2,c})^{0.5}}{P_{H_2O,c}}\right], \tag{8}$$

where E_0 is the standard electromotive force, T is the temperature, n is the number of electrons participating in a reaction, R and F are the gas constant and Faraday's constant, respectively, $P_{H_{2,a}}$ is the hydrogen partial pressure in the anode side, and $P_{O_{2,c}}$ and $P_{H2O,c}$ are the partial pressures of oxygen and water in the cathode side, respectively.

3.2.2 Concentration over-voltage

The anode side and cathode side over-voltages are expressed as follows:

$$\eta_{con,\alpha} = -\frac{RT}{\alpha_a 2F}\left(1 - \frac{i}{i_{L,H_2}}\right), \tag{9}$$

$$\eta_{con,c} = -\frac{RT}{\alpha_{1,c} 2F}\left(1 - \frac{i}{i_{L,O_2}}\right), \tag{10}$$

where α_a and $\alpha_{1,C}$ are the transfer coefficient of anode and cathode and correction coefficient as stated above. i_{L,H_2} and i_{L,O_2} are the limiting current densities and can be expressed as follows:

$$\begin{aligned} i_{L,H_2} &= nFf_a D_{H_2} \frac{C_{H_2,g}}{l} = 2Ff_a D_{H_2} \frac{1}{l} \frac{P_{H_2,g}}{RT} \\ i_{L,O_2} &= nFf_c D_{O_2} \frac{C_{O_2,g}}{l} = 4Ff_c D_{O_2} \frac{1}{l} \frac{P_{O_2,g}}{RT} \end{aligned} \tag{11}$$

where D is the diffusion coefficient and f is the effective porosity of the GDL. The current density i can be estimated from the hydrogen concentration gradient in the GDL. In fact, the hydrogen concentration in the GDL decreases on moving from the separator channel toward the MEA. Here we assume that the hydrogen concentration gradient is linear and constant in the GDL with a thickness of l, and the current density can then be obtained as

$$i = 2Ff_a \frac{C_{H_2,g} - C_{H_2,e}}{l}, \quad (12)$$

where $C_{H_2,g}$ is the molar concentration at the interface between the separator channel and the GDL, and $C_{H_2,e}$ is that on the surface of the catalyst layer.

3.2.3 Activation over-voltage

In this study, the activation over-voltage was calculated using the Butler–Volmer equation with the Tafel approximation:

$$\eta_{act} = \frac{RT}{\alpha_{2,c}} \ln \frac{i}{A_e \cdot i_0^+}, \quad (13)$$

where $\alpha_{2,c}$ is the transfer coefficient estimated by Parthasarathy et al.[19]:

$$\alpha_{2,c} = C_\alpha + 2.3 \times 10^{-3}(T - 303.15), \quad (14)$$

and A_e is the effective surface area per unit projected area of the electrode and can be calculated using the following equation:

$$A_e = m_{pt} A_s, \quad (15)$$

where m_{pt} is the amount of platinum per unit electrode area, and A_s is the effective surface area per unit of platinum. The term i_0^+ in Eq. (13) denotes the oxygen exchange current density and can be obtained from an equation suggested by Yoshikawa et al.[20]

3.2.4 Resistance over-voltage

In this study, the resistance over-voltage is expressed by the following equation:

$$\eta_{ohm} = \frac{t}{\sigma_{e,m}} i, \quad (16)$$

where t is the thickness of the electrolyte membrane. $\sigma_{e,m}$ is the ionic conductivity of the membrane, which can be calculated using Springer's model[21]:

$$\sigma_{e,m} = (0.00514\lambda - 0.00326) \cdot \exp\left[1268\left(\frac{1}{303} - \frac{1}{T}\right)\right], \quad (17)$$

The term λ in Eq. (17) is the anode side water content and can be expressed as a function of anode water activity ξ_a:

$$\lambda = \begin{cases} 0.043 + 17.8\xi_a - 38.9(\xi_a)^2 - 36.0(\xi_a)^3 & (\xi_a \le 1) \\ 14.1 + 1.4(\xi_a - 1) & (\xi_a > 1) \end{cases}. \quad (18)$$

ξ_a is obtained using the following equation:

$$\xi = \frac{x_{H_2O} P_a}{P_{H_2O(sat),a}}, \quad (19)$$

where x_{H_2O} is the molar fraction of water, and $P_{H_2O(sat),a}$ is the saturated vapor pressure calculated using the Antoine equation.

3.2.5 Hydrogen consumption rate

The rate of hydrogen consumption due to electrochemical reactions, S_{H2}, is calculated using the following equation:

$$S_{H_2} = \int \frac{i}{2F} dS, \quad (20)$$

where the integral is over a unit surface area of the catalyst. S_{H_2} is to calculate as a source term of boundaries.

3.3 Numerical Simulation System and Method

The numerical simulation model was developed based on OpenFOAM, which is an open-source CFD library.[22] The governing equations, Eqs. (1)–(6), were discretized by a finite volume method and solved using the PISO algorithm. In the analysis, advection terms were treated by a second-order upwind scheme and diffusion terms were treated by a second-order central differential scheme. The electrochemical reaction model was coupled with OpenFOAM. Hydrogen consumption due to the electrochemical reaction in the anode was considered as a boundary condition in the chemical species transport equations. The parameters used in the electrochemical reaction model are listed in Tables 1 and 2.

4. Results and Discussion

4.1 U-type Channel Flow: Comparison of CFD Results with Experimental Data

In this study, the water flow inside a U-type channel was calculated as shown in Fig. 2. The water temperature was 298 K, its kinematic viscosity was 1.004×10^{-6} m^2/s, and the average inlet velocity was 0.04 m/s. Figure 3 shows calculation results of the x-direction velocity, and the results of a laser Doppler velocimetry experiment performed by Taninaka et al. are also shown for comparison [23]. The calculation results of the CFD model show good agreement with the experimental data. This study confirmed that the CFD model is able to precisely predict serpentine flow-field characteristics.

4.2 Comparison of Calculation Results of PEFC Model with Experimental Data

To evaluate the electrochemical reaction model, performance tests were carried out in this study using pure hydrogen fuel gas, and the analyzed results were compared with the experimental data. Figure 4 shows a schematic of the PEFC performance test apparatus. Hydrogen and nitrogen were mixed by mass flow controllers to a prescribed concentration and flow rate before being supplied to the anode channel. At the same time, pure oxygen was supplied to the cathode channel. Both gases supplied to the anode and to the cathode were humidified so the PEFC operated in the wet state. The operating temperature was kept at 353 K during experiments, and the standard electromotive force was 0.5 V.

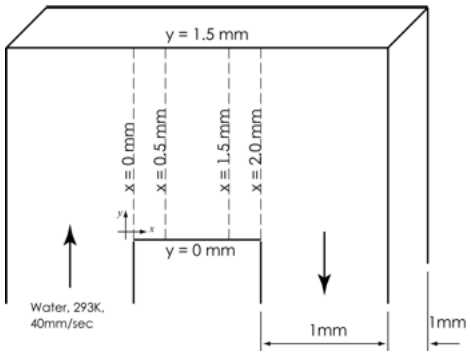

Figure 2. Schematic of U-type channel and LDV measurement points of experiment.

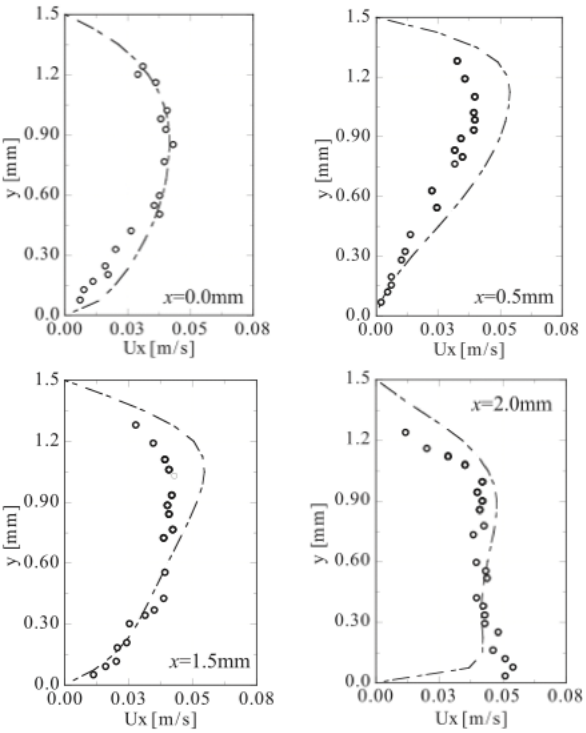

Figure 3. x-direction velocity comparisons between CFD result and LDV measurement data by Taninaka.et al.[23].

Figure 5 shows a comparison of the calculation results with experimental data in the case of pure hydrogen fuel. From the experimental results, the cell voltage gradually decreases as the current density increases. The calculation results obtained with the PEFC model show the same tendency as the experimental results but over a wider current density range. Based on these comparisons, the PEFC model developed in this study is able to predict PEFC performance reasonably well.

4.3 Effect of Hydrogen Concentration on Voltage/Current Density Using Electrochemical Reaction Model

The effect of hydrogen concentration on PEFC performance was investigated using the electrochemical reaction model. The operating voltage and fuel flow rate

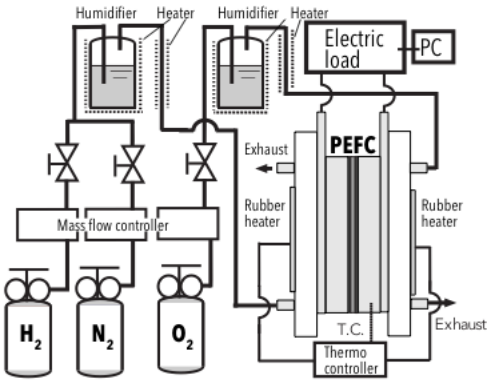

Figure 4. Experimental apparatus using JARI standard PEFC cell

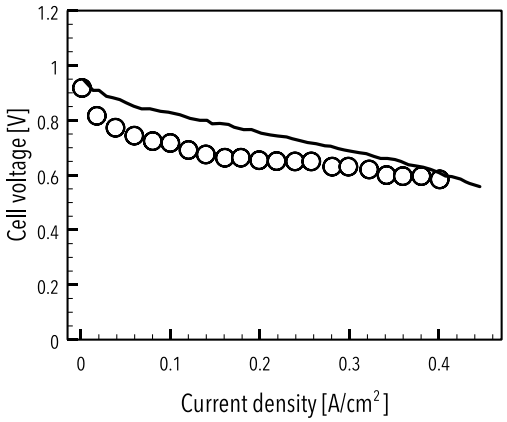

Figure 5. PEFC performance characteristics using pure hydrogen fuel: comparison between experiment and PEFC reaction model (temperature is 353K)

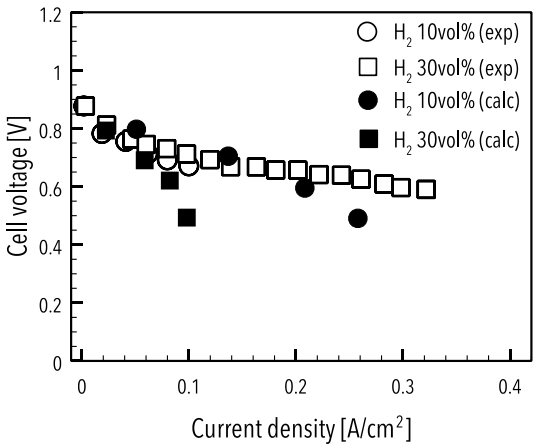

Figure 6. Comparison between results of experiment and of PEFC model; effect of hydrogen concentration on PEFC performance (fuel supply flow rate is 200sccm).

were set at 0.5 V and 200 sccm (standard cc per minute), respectively. Figure 6 shows the relationship between cell voltage and current density under two hydrogen concentration conditions, 10 and 30 vol.%. When the hydrogen concentration is 10 vol.%, the cell voltage rapidly decreases with increasing current density, unlike

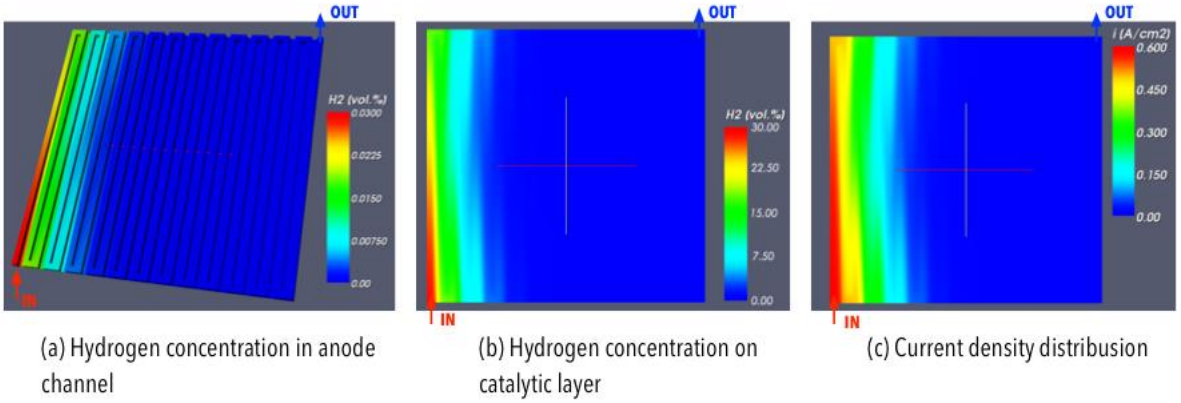

(a) Hydrogen concentration in anode channel (b) Hydrogen concentration on catalytic layer (c) Current density distribusion

Figure 7. Hydrogen distribution and current density distribution in anode side (fuel supply flow rate and its hydrogen concentration are 100sccm and 30%, respectively).

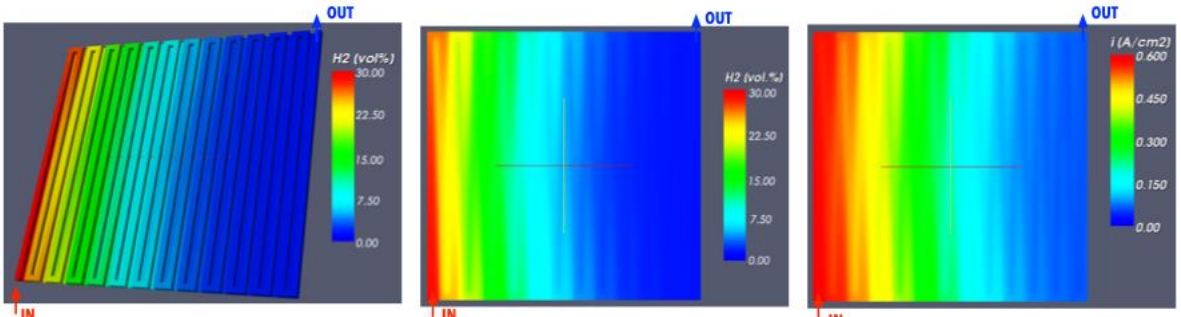

(a) Hydrogen concentration in anode channel (b) Hydrogen concentration on catalytic layer (c) Current density distribusion

Figure 8. Hydrogen distribution and current density distribution in anode side (fuel supply flow rate and its hydrogen concentration are 200sccm and 30%, respectively).

the results of pure hydrogen and 30 vol.% hydrogen. This characteristic is caused by concentration over-voltage arising from a depletion of hydrogen and reduced ion species at the electrode surface. By comparing with the experimental data, it is clear that the electrochemical reaction model developed in this study gives reasonable results even under low hydrogen concentration operating conditions.

4.4 Result of CFD Analysis for Anode Separator Channel: Hydrogen and Current Density Distributions under Low-Hydrogen Conditions

Figures 7 and 8 show hydrogen distributions and contour maps of current density on the catalyst layer surface, for which the calculation conditions were 30 vol.% hydrogen concentration in the fuel gas with a supply flow rate of 100 sccm and 200 sccm, respectively. The current density decreases from the inlet to the outlet, and the decrease is less under the higher flow rate condition. The performance degradation ratios relative to pure hydrogen are summarized in Table 3. As shown in the figures and the table, the hydrogen concentration and its distribution in the anode strongly affect the maximum current density. These results lead us to the conclusion that the degradation of PEFC performance caused by low hydrogen concentration is suppressed by forced convection of the fuel gas, even though the concentration is as low as 10 vol.%. In addition, geometrical optimization of the flow channel could promote a homogeneous hydrogen concentration distribution throughout the entire anode channel, consequently enhancing PEFC performance.

5. Conclusion

To evaluate the effect of low-hydrogen conditions on PEFC performance, this study developed a PEFC model that combines CFD analysis and a PEFC electrochemical reaction model, and the effects of low hydrogen concentration fuel gas and fuel supply flow rate were investigated using the model. The results indicate that the developed model is able to accurately predict PEFC performance under a wide range of hydrogen concentration conditions. The degradation of PEFC performance caused by low hydrogen concentration can be suppressed by the forced convection of fuel gas. This suppression implies that fuel gas with hydrogen

concentrations as low as 10 vol.% could be used in PEFCs by controlling the fuel supply flow rate. Furthermore, geometrical optimization of the separator channel should lead to a homogeneous hydrogen distribution in the anode, thus improving PEFC performance. The model developed in this study is useful in the optimizations of PEFC operating condition and separator channel design under low-hydrogen conditions.

Acknowledgement

This work was supported by the Research Foundation for Electro-Technology of Chubu and the Research Institute for Information Technology, Kyushu University. We gratefully acknowledge their support.

References

[1] Smitha B, Sridhar S, Khan A. Solid polymer electrolyte membranes for fuel cell applications; a review. J Membrane Science. 2005;259(1-2):10-26.

[2] Kothar R, Sawhney BR. Comparison of environmental and economic aspects of various hydrogen production methods. *Renewable and Sustainable Energy Reviews*. 2008;12(2):553-563.

[3] Navarro RM, Pena MA, Fierro JLG. Hydrogen production reactions from carbon feedstocks: Fossil fuels and biomass. *Chem Rev*. 2007;107(10):3952-3991.

[4] Majlan EH, Daud WR, Iyuke SE. Hydrogen purification using compact pressure swing adsorption system for fuel cell. Int J Hydrogen Energy. 2009;36(9):2771-2777.

[5] Yang T, Xiao Y, Chung TS. Poly-/metal-benzimidazole nano-composite membranes for hydrogen purification. Energy & Environmental Science. 2011;4(5):4171-4180.

[6] Konomi T, Sasaki Y. Effects of Running Condition on Over Voltage in PEFC. *Trans JSME Series B*. 2005;71(705): 1428-1435.

[7] Weng FB, Su A, Jung GB, Chiu YC, Chan SH. Numerical Prediction of Concentration and Current Distributions in PEFC. *J Power Sources*. 2005;145(2):546-554.

[8] Um S, Wang CY. Three-Dimensional Analysis of Transport and Electrochemical Reactions in Polymer Electrolyte Fuel Cells. *J Power Sources*. 2004;125(1):40-51.

[9] Stokie JM, Promislov K, Wetton BR. A Finite Volume Method for Multicomponent Gas Transport in Porous Fuel Cell Electrode. *Int J Numer Methods Fluids*. 2003;41(6):577-599.

[10] Wang Y, Wang CY. Ultra Large-Scale Simulation of Polymer Electrolyte Fuel Cells. *J Power Sources*. 2006;153(2):130-135.

[11] Gurau V, Mann JA. A critical overview of computational fluid dynamics multiphase models for proton exchange membrane fuel cells. *SIAM J Appl Math* 2009;70(2):410-454.

[12] Ferng YM, Su A. A three-dimmensional full-cell CFD model used to investigate the effect of different flow channel designs on PEMFC performance. Int J Hydrogen Energy 2007;32(17):4466-4476.

[13] Hashemi F, Rowshanzamir S, Rezakazemi M. CFD simulation of PEM fuel cell performance: effect of straight and serpentine flow fields. Math Comput Model 2012;55(3-4):1540-1557.

[14] Zhou T, Liu H. Effects of the electrical resistances of the GDL in a PEM fuel cell. J Power Sources 2006;161(1):444-453.

[15] Kopanidis A, Theodorakakos A, Gavaises M, Bouris D. Pore scale 3D modelling of heat and mass transfer in the gas diffusion layer and cathode channel of a PEM fuel cell. Int J Therm Sci 2011;50(4):456-467.

[16] Taymaz I, Benli M. Numerical study of assembly pressure effect on the performace of proton exchange membrane fuel cell. Energy 2010; 35(5):2134-2140.

[17] Inoue G, Matsukuma Y, Minemoto M. Evaluation of the Optimal Separator Shape with Reaction and Flow Analysis of Polymer Electrolyte Fuel Cell. *J Power Sources*. 2006;154(1):18-34.

[18] Inoue G, Matsukuma Y, Minemoto M. Effect of Gas Channel Depth on Current Density Distribution of Polymer Electrolyte Fuel Cell by Numerical Analysis Including Gas Flow Through Gas Diffusion Layer. *J Power Sources*. 2006;157(1):136-152.

[19] Parthasarathy A, Srinivasan S, Appleby J. Temperature Dependence of the Electrode Kinetics of Oxygen Reduction at the Platinum/Nafion Interface–a Microelectrode Investigation. *J Electrochem Soc*. 1992;139(5):2530-2537.

[20] Yoshikawa H, Hishinuma Y, Chikahisa T. Performance of a Polymer Electrolyte Fuel Cell for Automotive Applications. *Trans JSME Series B*. 2000;66(652):3218-3225.

[21] Springer TE, Zawodzinski TA, Gottesfeld S. Polymer Electrolyte Fuel Cell Model. *J Electrochem Soc*. 1991;138(8):2334-2342.

[22] Weller HG, Tabor G, Jasak H, Fureby CA. Tensorial Approach to Computational Continuum Mechanics Using Object-Oriented Techniques. *Comp Physics*. 1998;12(6):620-632.

[23] Taninaka S, Takada Y, Wakisaka T, Furuichi N, Toga S, Hachiga T. Investigation of the Shape of the Anode Flow Channel in a Direct Ethanol Polymer Electrolyte Fuel Cell. *J Environment and Engineering*. 2008;3(2):326-328